

Responses to Referee #1's comments

We are grateful to the reviewers for their valuable and helpful comments on our manuscript “**Molecular-level study on the role of methanesulfonic acid in iodine oxoacids nucleation**” (MS No.: egusphere-2023-2084). We have revised the manuscript carefully according to reviewers' comments. The point-to-point responses to the Referee #1's comments are summarized below:

Referee comments:

Li et al. explored the role of methanesulfonic acid (MSA) in iodine oxoacids nucleation. Detailed molecular-level mechanisms of cluster formation were studied using quantum chemical methods and cluster dynamics, providing theoretical evidence for the contribution of MSA to the formation of marine iodine clusters. After carefully reading the manuscript, I find that the main argument that MSA may enhance the nucleation rate of iodine oxoacids is convincing. The contribution of MSA to the formation of marine iodine particles remains an open question because other acids and bases such as sulfuric acid and amines may also affect the HIO_3 - HIO_2 nucleation process in the real atmosphere - as the authors have addressed at the end of this manuscript - while this study provides an important theoretical basis for this question. This manuscript is well written. I recommend it be accepted by *Atmospheric Chemistry and Physics*. A few minor comments on the interpretation of the theoretical results are given below.

Response: Thanks sincerely for the reviewer's professional and positive comments. We have revised the manuscript accordingly. The detailed point-to-point responses are listed as follows.

General comments:

Comment 1: Figures 1-3 seem to suggest that the significant enhancement of MSA on HIO_3 - HIO_2 nucleation is robust against the uncertainties of cluster stability. However, would it be possible to have a supplementary or appendix figure for the general audience, showing the uncertainty range of the enhancement or relative contribution of MSA to the cluster formation rate?

Response: Thanks for the reviewer's professional and helpful comments. The uncertainties of enhancement of MSA on cluster formation may stem from ACDC simulations and quantum

chemical (QC) calculations, thereby we examined how variable ACDC settings, such as condensation sink coefficient (CS), sticking factor (SF, corresponding to a sticking probability for cluster/monomer collision) and the change of calculated Gibbs free energy of cluster formation (ΔG , from quantum chemical calculations) impact the enhancement of MSA (R_{MSA}) on cluster formation rate (J). Here, the CS values ranged from $1.0 \times 10^{-4} \text{ s}^{-1}$ to $1.0 \times 10^{-2} \text{ s}^{-1}$, covering possible CS in relatively clean and polluted regions^[1,2]. The range of SF was set from 0.1 to 1.0 since sticking probabilities for neutral-neutral collisions between 0.1 and 1.0^[3].

As shown in the Figs. S15 (a) and (b), although both CS and SF affect R_{MSA} to some extent, the uncertainty range are relatively limited (CS < 32.5% and SF < 17.1%) and the results does not affect the trend and main conclusions.

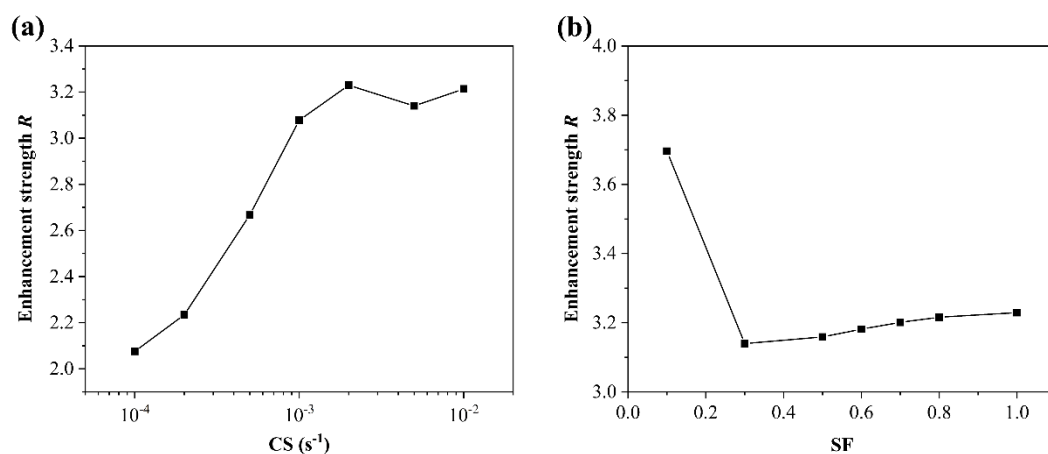


Figure S15. Variation of enhancement strength R of MSA with (a) condensation sink coefficient (CS) and (b) sticking factor (SF) for $\text{HIO}_3\text{-HIO}_2\text{-MSA}$ system at $T = 278 \text{ K}$, $[\text{HIO}_3] = 1.0 \times 10^7$, $[\text{HIO}_2] = 2.0 \times 10^5$, and $[\text{MSA}] = 1.0 \times 10^7 \text{ molec. cm}^{-3}$.

In addition, the potential uncertainty of quantum chemical calculations is ultimately manifested in the calculated ΔG values. As reported by Kupiainen^[4] et al. (2012), the differences between the computational (DFT//RI-CC2 method) and experimental ΔG values are about 1 kcal mol^{-1} or less^[5]. Accordingly, Almedia^[3] et al. (2013) calculated the uncertainty range of ACDC simulated cluster formation resulting from QC calculations by adjusting the binding energy ($\pm 1 \text{ kcal mol}^{-1}$). Further given the consistency of our research framework (DFT//RI-CC2 + ACDC) with Almedia et al. (2013), herein we have performed the uncertainty analysis of R_{MSA} caused by QC calculations through adding or subtracting 1 kcal mol^{-1} from the ΔG (using $\Delta G_{278\text{K}}$ as a reference). The figure below presents the uncertainty analysis results of

J and R_{MSA} at $T = 278$ K, $\text{CS} = 2.0 \times 10^{-3} \text{ s}^{-1}$, $[\text{HIO}_3] = 10^7$, $[\text{HIO}_2] = 2.0 \times 10^5$, $[\text{MSA}] = 10^6 - 10^8 \text{ molec. cm}^{-3}$.

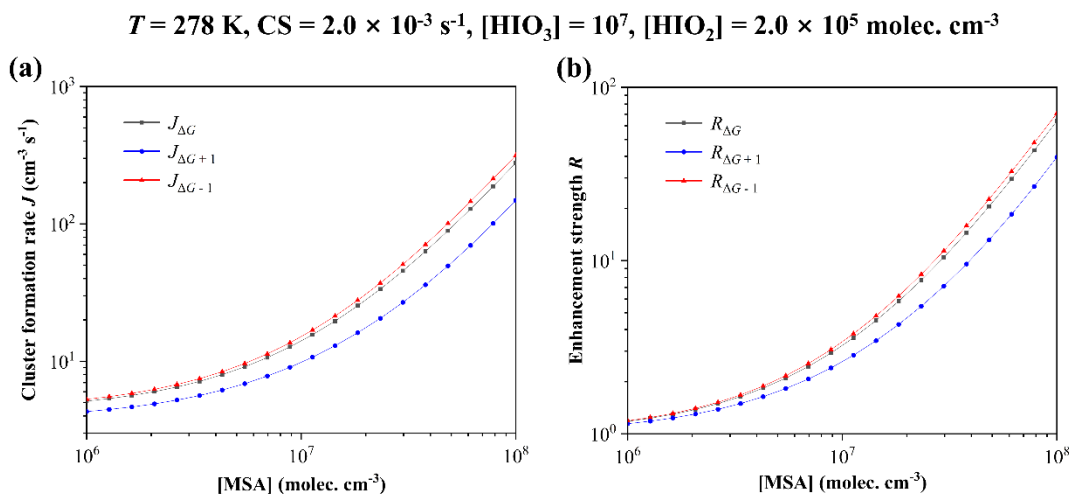


Figure S16. Cluster formation rate J (a) and enhancement strength R of MSA (b) as a function of $[\text{MSA}] = 10^6 - 10^8 \text{ molec. cm}^{-3}$, with different energy of $\Delta G_{278\text{K}}$ (black line), $\Delta G_{278\text{K}} + 1$ (blue line), $\Delta G_{278\text{K}} - 1$ (red line), at $T = 278$ K, $\text{CS} = 2.0 \times 10^{-3} \text{ s}^{-1}$, $[\text{HIO}_3] = 10^7$, $[\text{HIO}_2] = 2.0 \times 10^5 \text{ molec. cm}^{-3}$.

Here, we have added the results of R_{MSA} under different CS, SF and ΔG to the revised supporting file, and for the convenience of the review, we have copied Figures S15-S16 and the corresponding analysis as following: “Here, the potential uncertainties may stem from ACDC simulations and quantum chemical (QC) calculations, we examined the effect of condensation sink coefficient (CS), sticking factor (SF) and calculated ΔG of clusters on enhancement of MSA to the cluster formation rate. The CS values ranged from $1.0 \times 10^{-4} \text{ s}^{-1}$ to $1.0 \times 10^{-2} \text{ s}^{-1}$, covering possible CS in relatively clean and polluted regions^[1, 2]. The range of SF was set from 0.1 to 1.0 since sticking probabilities for neutral-neutral collisions between 0.1 and 1.0^[3]. Both the CS and SF slightly affect the enhancement of MSA, with limited uncertainty range of $\text{CS} < 32.5\%$ and $\text{SF} < 17.1\%$ (Fig. S15). As reported by Kupiainen^[4] et al. (2012), the differences between the computational (DFT//RI-CC2 method) and experimental ΔG values are about 1 kcal mol^{-1} or less^[5]. Accordingly, Almedia^[3] et al. (2013) calculated the uncertainty range of ACDC simulated cluster formation resulting from QC calculations by adjusting the binding energy ($\pm 1 \text{ kcal mol}^{-1}$). Further given the consistency of our research framework (DFT//RI-CC2 + ACDC) with Almedia et al. (2013), herein we have performed the uncertainty

analysis of R_{MSA} caused by QC calculations through adding or subtracting 1 kcal mol⁻¹ from the ΔG (using $\Delta G_{278\text{K}}$ as a reference). As shown in Table S8 and Fig. S16, adjusting the $\Delta G_{278\text{K}}$ of clusters by ± 1 kcal mol⁻¹ resulted in a minor variation in J and R of MSA, with the overall trend remaining consistent.”

Comment 2: I found it challenging to interpret the relative importance of the MSA-involved path in HIO₃-HIO₂-MSA nucleation. Figure 3a shows that the MSA-involved path is a major path (74 %), yet this was simulated with a [MSA] 5 times of [HIO₃]. With the same [MSA] and [HIO₃], the MSA-involved path was expected to contribute ~20 %, showing that MSA was a bit less efficient than HIO₃ in clustering with HIO₂. This comparatively lower efficiency does not affect the main conclusion as the [MSA] may exceed [HIO₃] in atmospheric environments. However, Figures 4 and 5 show a high enhancement factor (> 2) with the same [MSA] and [HIO₃]. This high enhancement factor indicates that MSA is more efficient than what I interpreted above. I hope this can be clarified in the revised manuscript.

Response: This is a very insightful point – thanks for bringing it up. Indeed, as expertly assessed by the reviewer, HIO₃ undergo clustering with HIO₂ more efficiently than MSA due to the lower contribution of MSA-involved pathway (~20%) at same concentrations of HIO₃ and MSA (10⁷ molec. cm⁻³). However, in this case, the involvement of MSA in nucleation shows a high enhancement factor (> 2) for rate J , which is indeed the point that may confuse the reader. Accordingly, we explored the underlying nucleation mechanism under the focused condition: $T = 278\text{K}$, $CS = 2.0 \times 10^{-3} \text{ s}^{-1}$, (a) $[\text{HIO}_3] = [\text{MSA}] = 1.0 \times 10^7$, and $[\text{HIO}_2] = 2.0 \times 10^5$ molec. cm⁻³. (b) $[\text{HIO}_3] = [\text{MSA}] = 1.0 \times 10^6$, and $[\text{HIO}_2] = 2.0 \times 10^4$ molec. cm⁻³.

As shown in Fig. S7, the contribution of MSA to clustering consists not only of directly forming HIO₃-HIO₂-MSA clusters (~20%), but also its ‘catalysis’ role in facilitating formation of initial HIO₃-HIO₂ clusters, e.g., (HIO₃)₁(HIO₂)₁₋₂, through a process of first participation in forming the (HIO₃)₁(HIO₂)₁₋₂(MSA)₁ clusters, and then evaporation out. Taken together, MSA promotes both HIO₃-HIO₂-MSA and HIO₃-HIO₂ clustering pathways, and its dual contribution results in a high enhancement factor (> 2).

Furthermore, to make the readers clear, we accordingly provide an explanatory account of this phenomenon as follows (Lines 227-231 in the revised manuscript): “However, the

atmospheric $[\text{HIO}_3]$ ranges widely from 10^6 to 10^8 molec. cm^{-3} . When $[\text{HIO}_3]$ is comparable or higher than $[\text{MSA}]$, the HIO_3 - HIO_2 pathway contributes more, and the R of MSA decreases with the rising $[\text{HIO}_3]$. It is worth noting that when $[\text{HIO}_3]$ is comparable to $[\text{MSA}]$, the R of MSA is greater than 2, as the contribution of MSA to clustering includes not only the direct formation of HIO_3 - HIO_2 -MSA clusters ($\sim 20\%$), but also its ‘catalysis’ role in facilitating formation of initial HIO_3 - HIO_2 clusters (Fig. S7).”

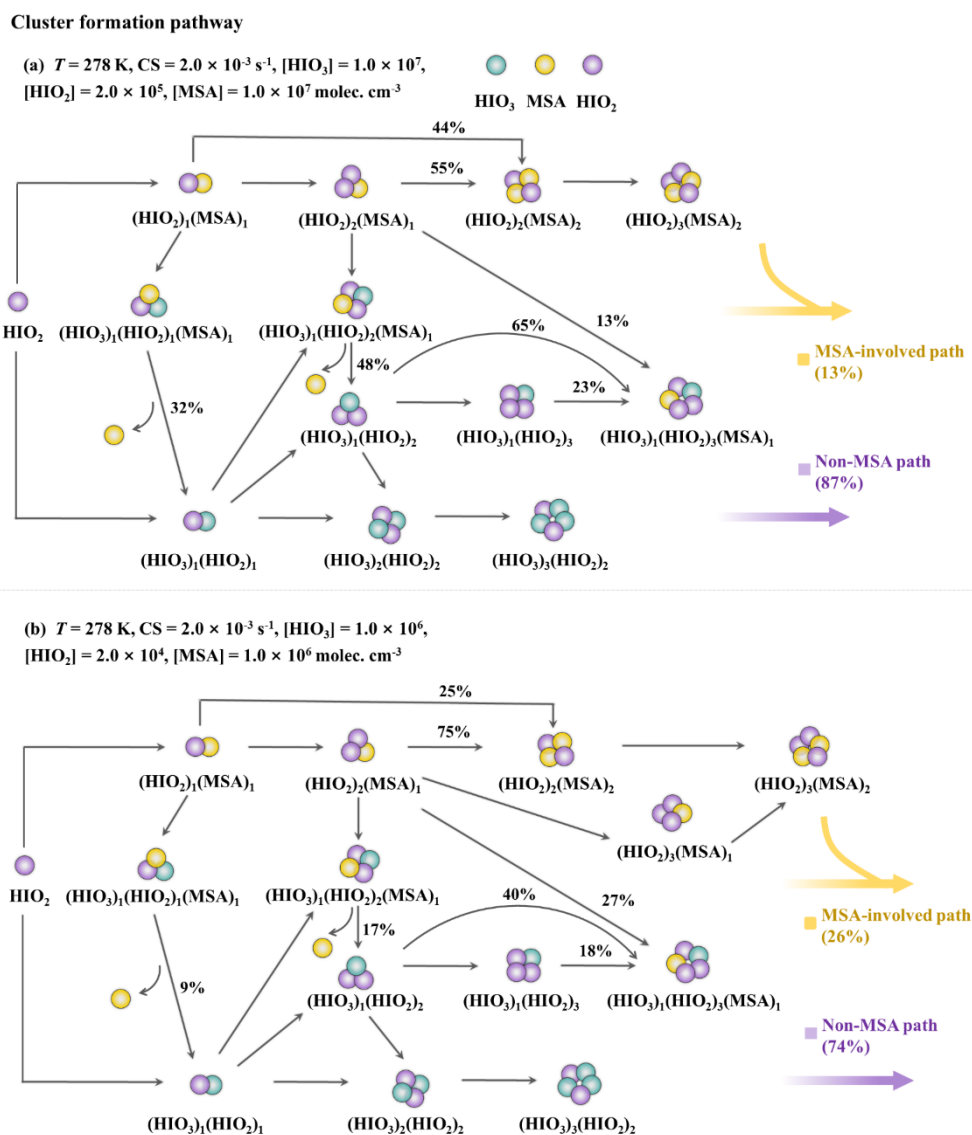


Figure S7. Main cluster growth pathway of the HIO_3 - HIO_2 -MSA nucleating system at $T = 278\text{K}$, $\text{CS} = 2.0 \times 10^{-3} \text{ s}^{-1}$, (a) $[\text{HIO}_3] = 1.0 \times 10^7$, $[\text{HIO}_2] = 2.0 \times 10^5$, and $[\text{MSA}] = 1.0 \times 10^7$ molec. cm^{-3} , (b) $[\text{HIO}_3] = 1.0 \times 10^6$, $[\text{HIO}_2] = 2.0 \times 10^4$, and $[\text{MSA}] = 1.0 \times 10^6$ molec. cm^{-3} .

Specific comments:

Comment 3: Line 180, "Overall, the results suggest that MSA's contribution to cluster formation is positively related to [MSA] but negatively linked to [HIO₃]." This sentence is correct in terms of the relative contribution but awkward. How about removing this sentence and adding discussions on the relative importance of the MSA path (see comment 2)?

Response: According to the reviewer's helpful suggestion, we have removed the mentioned sentence "Overall, the results suggest that MSA's contribution to cluster formation is positively related to [MSA] but negatively linked to [HIO₃]" in Line 180, and added the discussion of comment 2 in the revised manuscript (Lines 227-231, page 10).

Comment 4: Line 207, "To sum up, MSA can promote nucleation, particularly in marine regions characterized by lower T, lower [HIO₃] and [HIO₂]." I was confused that MSA can promote nucleation at low [HIO₂] within the context of this manuscript, as [HIO₂] is the starting point of cluster formation. This might be caused by overemphasizing the relative contribution. Also, [HIO₂] is usually associated with [HIO₃]. Replacing [HIO₃] (implicitly indicated to be independent of [HIO₂]) with [HIO₃]/[HIO₂] in some discussions may help with understanding.

Response: Certainly, as predicted by the reviewer, [HIO₂] is the starting point of cluster formation. When [HIO₂] declines, both MSA-involved and non-MSA pathway proportions decrease (see Fig. (3) in the main text). However, in this study, we draw the following conclusions based on the calculated enhancement strength (R) of MSA on nucleation, i.e., $R = J(\text{HIO}_3\text{-HIO}_2\text{-MSA}) / J(\text{HIO}_3\text{-HIO}_2)$. As [HIO₂] declines, both the numerator and denominator of R decrease. However, the numerator diminishes relatively slowly due to the introduction of MSA, enhancing the rate and retarding its decay, which results in an increased R value. Yet, in environments with higher [HIO₂], the enhancing effect of MSA will be weaker because the more efficient HIO₃ will fully combine with HIO₂, thereby resulting in a lower R .

Accordingly, following the professional advice of the reviewer, to make it clear to the readers, we add the explanation prior to the introduction of the ACDC simulations as follows: "...where [HIO₃]/[HIO₂] is a constant" in Line 150 of page 6.

Comment 5: Line 222, "observed J of $2.1 \times 10^{-4} \text{ cm}^{-3} \text{ s}^{-1}$ ". This J value is too low from a

measurement point of view. In a scatter plot showing the correlation between J and precursor concentrations, some small values of J are often given, though they might be obtained during weak or non-NPF periods. I checked the SI of Beck et al. and found that they have clarified that "Data with J -values $<$ a few $10^{-3} \text{ cm}^{-3} \text{ s}^{-1}$ are highly unreliable and reflect mainly the noise levels...". Figure 2a in their main manuscript shows that the J value is $\sim 0.1 \text{ cm}^{-3} \text{ s}^{-1}$ during typical NPF events.

Response: Thanks for these professional and rigorous suggestions. Accordingly, given the unreliability of J -values ($<$ a few $10^{-3} \text{ cm}^{-3} \text{ s}^{-1}$), we have adjusted the range of the observed cluster formation rate J of Ny-Ålesund to $10^{-3} - 10^{-1} \text{ cm}^{-3} \text{ s}^{-1}$ in Fig. 6(a). And the sentence "...the $J(\text{HIO}_3\text{-HIO}_2\text{-MSA})$ can be two orders of magnitude higher than the observed J of $2.1 \times 10^{-4} \text{ cm}^{-3} \text{ s}^{-1}$ " has been changed to "...the $J(\text{HIO}_3\text{-HIO}_2\text{-MSA})$ can be one order of magnitude higher than the observed J of $10^{-3} \text{ cm}^{-3} \text{ s}^{-1}$ " in Lines 248-249 (page 11) of the revised manuscript.

Comment 6: Figure 6. It is recommended to adjust the shaded area of field observation. Now the measured J shares a similar style with the simulated J . Some readers may wonder why there is no correlation between the measured J and $[\text{HIO}_3]$.

Response: Thanks. The reviewers' suggestion is helpful in improving the clarity of the data. Accordingly, we have changed the measured J with a different style in Fig. 6 from shaded areas to dashed lines.

Comment 7: Figure 6 caption. Please explain why there is a single line for $\text{HIO}_3\text{-HIO}_2$ while $[\text{HIO}_2]$ ranges from $2\text{e}3$ to $2\text{e}4$. Is it because of a constant $[\text{HIO}_2]/[\text{HIO}_3]$ in the simulation?

Response: As the reviewer's expert insight suggests, the reason that the rate of $\text{HIO}_3\text{-HIO}_2$ cluster formation presents as a line that increases with $[\text{HIO}_3]$ is that $[\text{HIO}_3]/[\text{HIO}_2]$ is fixed to a constant value (50, according to the field measured ratio from Sipilä et al. 2016^[6]) in the simulation. To make it clearer for the readers, we have added a description of the relationship between $[\text{HIO}_3]$ and $[\text{HIO}_2]$ to the caption of Fig.6 as: " $[\text{HIO}_3]/[\text{HIO}_2]$ is a constant".

Comment 8: Figure S5. Please give the reference for field observation data herein. It is surprising to see a high formation rate of $1\text{e}4\text{-}1\text{e}6 \text{ cm}^{-3} \text{ s}^{-1}$.

Response: According to the reviewer's suggestion, the corresponding reference (O'Dowd, et al., *J. Geophys. Res.: Atmos.*, 2002)^[7] has been cited in the caption of Figure S14 (previous Figure S5) in the revised supporting information.

Comment 9: Line 248, "...thermodynamic analyses suggest that MSA-involved clustering is nearly barrierless". I do not disagree with this statement, yet it may confuse some readers, especially considering that the horizontal axes in Figs. 5-6 are [HIO₃] rather than [HIO₂]. How about emphasizing that the HIO₂ addition, as the rate-limiting step for cluster formation and growth, is nearly barrierless?

Response: Thanks for the reviewer's professional comments. The preference for [HIO₃] as the horizontal axes in Figs. 5-6 is due to the strong correlation between NPF occurrence and observations of iodic acid^[6]. Also, in CLOUD experiments, the nucleation rates show a strong dependency on HIO₃ concentration^[8]. Conversely, there are limited available field observations of HIO₂, characterized by lower reported concentrations, despite its pivotal role in stabilizing HIO₃ cluster. Therefore, the concentration of HIO₃ is employed here as horizontal axes to present the results of cluster formation rate or enhancement strength.

Furthermore, as mentioned by the reviewer, the HIO₂ addition is the rate-limiting step for cluster formation, which leads to the significant increasement of the $J(\text{HIO}_3\text{-HIO}_2\text{-MSA})$ compared to $J(\text{HIO}_3\text{-MSA})$ (Figure S12). As shown in Figure S13, thermodynamic analysis suggest that compared with HIO₃-MSA pathway, HIO₃-HIO₂-MSA path is almost barrierless (1.24 kcal mol⁻¹) at $T = 278$ K, $[\text{HIO}_3] = 1.0 \times 10^6$, $[\text{HIO}_2] = 2.0 \times 10^4$, and $[\text{MSA}] = 5.0 \times 10^6$ molec. cm⁻³, indicating that the HIO₂ addition is favorable. To make the readers clear, we accordingly copy the explanation as follows (Lines 235-238 in the revised manuscript): "Furthermore, the effect of HIO₂ addition on the whole nucleation system was considered, as it is not only the rate-limiting step for cluster formation, leading to the significant increasement of the $J(\text{HIO}_3\text{-HIO}_2\text{-MSA})$ compared to $J(\text{HIO}_3\text{-MSA})$ (Figure S12), but also thermodynamically favorable due to HIO₃-HIO₂-MSA path is almost barrierless (1.24 kcal mol⁻¹) compared to HIO₃-MSA pathway (Figure S13)."

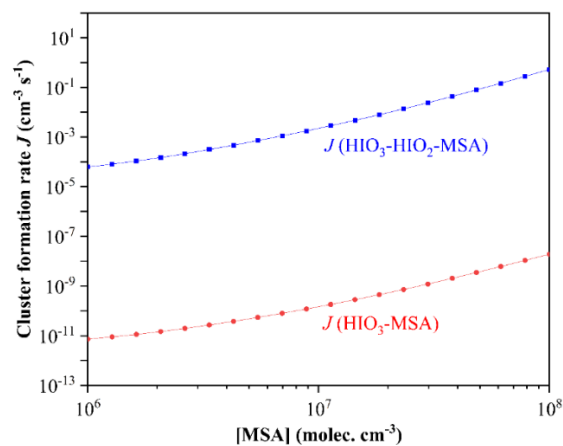


Figure S12. Simulated cluster formation rates J ($\text{cm}^3 \text{s}^{-1}$) against varying $[\text{MSA}] = 10^6 - 10^7$ molec. cm^{-3} , at $T = 278$ K, $\text{CS} = 2.0 \times 10^{-3} \text{ s}^{-1}$, $[\text{HIO}_3] = 1.0 \times 10^6$, $[\text{HIO}_2] = 2.0 \times 10^4$ molec. cm^{-3} .

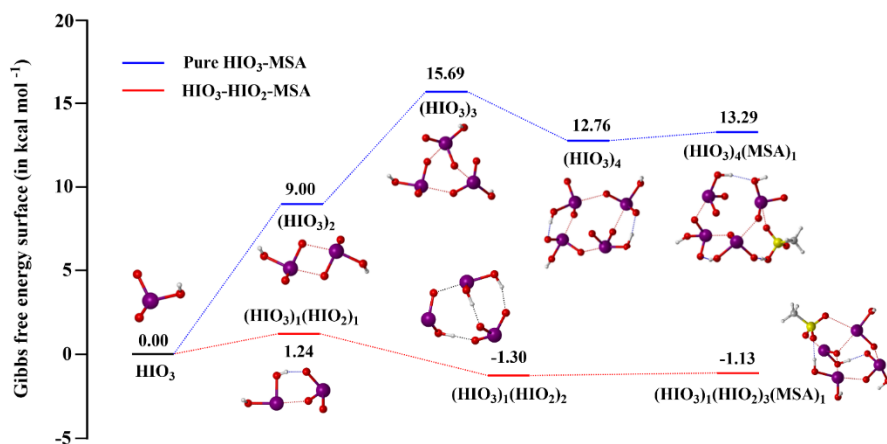


Figure S13. The Gibbs free energies of cluster formation (ΔG , kcal mol^{-1}) based on the main clustering pathway in HIO_3 -MSA and HIO_3 - HIO_2 -MSA nucleation system at $T = 278$ K, $\text{CS} = 2.0 \times 10^{-3} \text{ s}^{-1}$, $[\text{HIO}_3] = 1.0 \times 10^6$, $[\text{HIO}_2] = 2.0 \times 10^4$ molec. cm^{-3} .

Reference:

- [1] X.-C. He, Y.J. Tham, L. Dada, M. Wang, H. Finkenzeller, D. Stolzenburg, S. Iyer, M. Simon, A.K. Kürten, J. Shen, B. Roerup, M. Rissanen, S. Schobesberger, R. Baalbaki, D.S. Wang, T.K. Koenig, T. Jokinen, N. Sarnela, L.J. Beck, J. Almeida, S. Amanatidis, A. Amorim, F. Ataei, A. Baccarini, B. Bertozzi, F. Bianchi, S. Brilke, L. Caudillo, D. Chen, R. Chiu, B. Chu, A. Dias, A. Ding, J. Dommen, J. Duplissy, I.E. Haddad, L.G. Carracedo, M. Granzin, A. Hansel, M. Heinritzi, V. Hofbauer, H. Junninen, J. Kangasluoma, D. Kemppainen, C. Kim, W. Kong, J.E. Krechmer, A. Kvashin, T. Laitinen, H. Lamkaddam, C.P. Lee, K. Lehtipalo, M. Leiminger, Z. Li, V. Makhmutov, H.E. Manninen, G. Marie, R. Marten, S. Mathot, R.L. Mauldin, B. Mentler, O. Moehler, T. Mueller, W. Nie, A. Onnela, T. Petaja, J. Pfeifer, M. Philippov, A. Ranjithkumar, A. Saiz-Lopez, I. Salma, W. Scholz, S. Schuchmann, B. Schulze, G. Steiner, Y. Stozhkov, C. Tauber, A. Tome, R.C. Thakur, O. Vaisanen, M. Vazquez-Pufleau, A.C. Wagner, Y. Wang, S.K. Weber, P.M. Winkler, Y. Wu, M. Xiao, C. Yan, Q. Ye, A. Ylisirmio, M. Zauner-Wieczorek, Q. Zha, P. Zhou, R.C. Flagan, J. Curtius, U. Baltensperger, M. Kulmala, V.-M. Kerminen, T. Kurten, N.M. Donahue, R. Volkamer, J. Kirkby, D.R. Worsnop, M. Sipila, Role of iodine oxoacids in atmospheric aerosol nucleation, *Science* 371 (2021) 589–595.
- [2] H. Yu, L. Ren, X. Huang, M. Xie, J. He, H. Xiao, Iodine speciation and size distribution in ambient aerosols at a coastal new particle formation hotspot in China, *Atmos. Chem. Phys.* 19 (2019) 4025–4039.
- [3] J. Almeida, S. Schobesberger, A. Kürten, I.K. Ortega, O. Kupiainen-Määttä, A.P. Praplan, A. Adamov, A. Amorim, F. Bianchi, M. Breitenlechner, A. David, J. Dommen, N.M. Donahue, A. Downard, E. Dunne, J. Duplissy, S. Ehrhart, R.C. Flagan, A. Franchin, R. Guida, J. Hakala, A. Hansel, M. Heinritzi, H. Henschel, T. Jokinen, H. Junninen, M. Kajos, J. Kangasluoma, H. Keskinen, A. Kupc, T. Kurten, A.N. Kvashin, A. Laaksonen, K. Lehtipalo, M. Leiminger, J. Leppä, V. Loukonen, V. Makhmutov, S. Mathot, M.J. McGrath, T. Nieminen, T. Olenius, A. Onnela, T. Petäjä, F. Riccobono, I. Riipinen, M. Rissanen, L. Rondo, T. Ruuskanen, F.D. Santos, N. Sarnela, S. Schallhart, R. Schnitzhofer, J.H. Seinfeld, M. Simon, M. Sipilä, Y. Stozhkov, F. Stratmann, A. Tomé, J. Tröstl, G. Tsagkogeorgas, P. Vaattovaara, Y. Viisanen, A. Virtanen, A. Vrtala, P.E. Wagner, E. Weingartner, H. Wex, C. Williamson, D. Wimmer, P. Ye, T. Yli-Juuti, K.S. Carslaw, M. Kulmala, J. Curtius, U. Baltensperger, D.R. Worsnop, H. Vehkamäki, J. Kirkby, Molecular understanding of sulphuric acid-amine particle nucleation in the atmosphere, *Nature* 502 (2013) 359–363.
- [4] O. Kupiainen, I.K. Ortega, T. Kurtén, H. Vehkamäki, Amine substitution into sulfuric acid – ammonia clusters, *Atmos. Chem. Phys.* 12 (2012) 3591-3599.
- [5] K.D. Froyd, E.R. Lovejoy, Bond energies and structures of ammonia-sulfuric acid positive cluster ions, *J. Phys. Chem. A* 116 (2012) 5886-5899.
- [6] M. Sipilä, N. Sarnela, T. Jokinen, H. Henschel, H. Junninen, J. Kontkanen, S. Richters, J. Kangasluoma, A. Franchin, O. peräkylä, M.P. Rissanen, M. Ehn, H. Vehkamäki, T. Kurten, T. Berndt, T. Petäjä, D. Worsnop, D. Ceburnis, V.M. Kerminen, M. Kulmala, C. O'Dowd, Molecular-scale evidence of aerosol particle formation via sequential addition of HIO₃, *Nature* 537 (2016) 532–534.
- [7] C.D. O'Dowd, K. Hämeri, J. Mäkelä, M. Väkeva, P. Aalto, G. de Leeuw, G.J. Kunz, E. Becker, H.C. Hansson, A.G. Allen, R.M. Harrison, H. Berresheim, C. Kleefeld, M. Geever, S.G. Jennings, M. Kulmala, Coastal new particle formation: Environmental conditions and aerosol physicochemical characteristics during nucleation bursts, *J. Geophys. Res.-Atmos.* 107 (2002).
- [8] X.-C. He, S. Iyer, M. Sipilä, A. Ylisirmio, M. Peltola, J. Kontkanen, R. Baalbaki, M. Simon, A. Kürten, Y.J. Tham, J. Pesonen, L.R. Ahonen, S. Amanatidis, A. Amorim, A. Baccarini, L. Beck, F. Bianchi, S. Brilke, D. Chen, R. Chiu, J. Curtius, L. Dada, A. Dias, J. Dommen, N.M. Donahue, J. Duplissy, I. El

Haddad, H. Finkenzeller, L. Fischer, M. Heinritzi, V. Hofbauer, J. Kangasluoma, C. Kim, T.K. Koenig, J. Kubečka, A. Kvashnin, H. Lamkaddam, C.P. Lee, M. Leiminger, Z. Li, V. Makhmutov, M. Xiao, R. Marten, W. Nie, A. Onnela, E. Partoll, T. Petäjä, V.-T. Salo, S. Schuchmann, G. Steiner, D. Stolzenburg, Y. Stozhkov, C. Tauber, A. Tomé, O. Väisänen, M. Vazquez-Pufleau, R. Volkamer, A.C. Wagner, M. Wang, Y. Wang, D. Wimmer, P.M. Winkler, D.R. Worsnop, Y. Wu, C. Yan, Q. Ye, K. Lehtinen, T. Nieminen, H.E. Manninen, M. Rissanen, S. Schobesberger, K. Lehtipalo, U. Baltensperger, A. Hansel, V.-M. Kerminen, R.C. Flagan, J. Kirkby, T. Kurtén, M. Kulmala, Determination of the collision rate coefficient between charged iodine acid clusters and iodine acid using the appearance time method, *Aerosol Sci. Tech.* 55 (2021) 231-242.